Combustion and Flame 194 (2018) 175–179

Contents lists available at ScienceDirect

Combustion and Flame

journal homepage: www.elsevier.com/locate/combustflame

Effects of Soret diffusion on premixed flame propagation under engine-relevant conditions

Mahdi Faghih[a], Wang Han[b], Zheng Chen[a,*]

[a] SKLTCS, Department of Mechanics and Engineering Science, College of Engineering, Peking University, Beijing 100871, China
[b] Institute for Simulation of reactive Thermo-Fluid Systems, TU Darmstadt, Darmstadt 64287, Germany

ARTICLE INFO

Article history:
Received 15 November 2017
Revised 27 April 2018
Accepted 28 April 2018

Keywords:
Soret diffusion
Laminar flame speed
Hydrogen/air
Engine-relevant conditions

ABSTRACT

Recent studies have shown that Soret diffusion has strong impact on the laminar flame speed of hydrogen/air mixture while it has little influence for hydrocarbon fuels at normal temperature and pressure. However, it is not clear whether the same conclusions hold under engine-relevant conditions. This is investigated in the present study. A series of premixed spherical flames propagating at high temperatures and pressures are simulated for different fuels, and the corresponding laminar flame speeds with and without considering Soret diffusion are obtained. It is found that for hydrogen/air mixture, Soret diffusion has much stronger influence on burning rate at engine-relevant conditions than at normal temperature and pressure. However, for hydrocarbon fuels like methane and iso-octane, Soret diffusion still has negligible effects on the burning rate even under engine-relevant conditions.

1. Introduction

It is well known that laminar premixed flame propagation is controlled by heat conduction and mass diffusion [1]. Mass diffusion mainly includes (1) Fickian diffusion due to concentration gradient and (2) Soret diffusion driven by temperature gradient [1,2]. Usually only the Fickian diffusion is considered in combustion modeling since it is the dominant mode of mass diffusion. However, under certain conditions (e.g., in the presence of very light species and very large temperature gradient), Soret diffusion cannot be neglected [3,4].

As reviewed in [3–5], there are many studies assessing Soret diffusion effects on laminar premixed flames. For examples, numerical simulation was conducted to assess Soret diffusion effects on the laminar flame speeds (LFSs) of different fuels (e.g., [6–12]). For hydrogen and syngas, LFS was shown to be reduced after considering Soret diffusion. This was found to be mainly due to the coupling between Soret diffusion of H radical and the chain branching reaction $H+O_2=O+OH$ [9,12]. For hydrocarbon fuels such as methane, n-butane and n-heptane, the influence of Soret diffusion on LFS was shown to be negligible [8,10,11]. Theoretical analysis considering Soret diffusion [13–15] was also conducted for laminar premixed flames. It was found that Soret diffusion modifies the local equivalence ratio and thereby affects the flame propagation speed. Besides premixed flames, Soret diffusion effects on diffusion flames were also investigated. Detailed description can be found in the recent reviews [3,4].

In previous studies, Soret diffusion effects were usually investigated under normal temperature and pressure (i.e., 298 K and 1 atm). Recently, Liang et al. [12] and Zhou et al. [16] have studied Soret diffusion effects at elevated temperatures and pressures examined. However, the elevated temperature and pressure, 500 K and 5 atm, considered in these studies are still far from engine-relevant conditions. It is still not clear whether Soret diffusion still has strong (negligible) impact on hydrogen (hydrocarbon) flames under engine-relevant conditions. The objective of this study is to answer this question. To this end, a series of premixed spherical flames propagating at high temperatures and pressures are simulated for different fuels. The corresponding LFSs with and without considering Soret diffusion are obtained, and then Soret diffusion effects on premixed flame propagation under engine-relevant conditions are assessed.

2. Numerical methods

Laminar flame speeds (LFSs) at elevated temperatures and pressures close to engine-relevant conditions are calculated through the constant-volume propagating spherical flame method (see [17] and references therein). In this method, a propagating spherical flame is initiated by spark ignition at the center of a closed spherical vessel. The evolution of chamber pressure rather than the flame radius is recorded. The pressure history, $P=P(t)$, is then used

* Corresponding author.
E-mail addresses: cz@pku.edu.cn, chenzheng@coe.pku.edu.cn (Z. Chen).

https://doi.org/10.1016/j.combustflame.2018.04.031
0010-2180/

to determine LFS through the following expression [17]:

$$S_u = \frac{R_W}{3}\left(1-(1-x)\left(\frac{P_0}{P}\right)^{1/\gamma_u}\right)^{-2/3}\left(\frac{P_0}{P}\right)^{1/\gamma_u}\frac{dx}{dt}, \quad (1)$$

where R_W is the radius of the spherical vessel, P_0 the initial pressure, and γ_u the heat capacity ratio of unburned gas. The burned mass fraction, x, is determined from pressure history through two-zone or multi-zone models in experiments (e.g., [18–20]) and it can be calculated directly in simulation. Readers who are interested in this method are referred to the Supplementary Document, which provides the detailed description of this method and detailed derivation of Eq. (1).

Compared to the other spherical flame method imaging flame front propagation (see [21] and references therein), the constant-volume propagating spherical flame method has the advantages that LFS for a given mixture over a broad range of temperatures and pressures can be simultaneously obtained from a single test and that it can be used to get LFS at engine-relevant temperatures and pressures [18]. Therefore, the constant-volume propagating spherical flame method is used here to calculate LFSs for different fuels with and without considering Soret diffusion. CHEMKIN-PREMIX code [22] is not used to calculate LFSs since it is difficult to get converged solutions at high temperatures and pressures.

One-dimensional premixed spherical flame propagating in a closed spherical vessel is simulated using the in-house code A-SURF (Adaptive Simulation of Unsteady Reactive Flow) [23–25]. Finite volume method is used to solve the conservation equations for compressible reactive flow. The CHEMKIN package [26] is incorporated into A-SURF to calculate thermal and transport properties and reaction rates. Three fuels, hydrogen, methane and iso-octane, are considered here. The detailed chemical mechanism developed by Li et al. [27] and GRI-Mech 3.0 [28] are used for hydrogen and methane, respectively. For iso-octane, the reduced mechanism in [29] is used. A-SURF has been used in previous studies on flame and detonation propagation (e.g., [30–34]). The detailed description of governing equations, numerical algorithms and code validation can be found in [23–25]. Here only the description of mass diffusion is presented.

The diffusion velocity of species k is composed of three parts:

$$V_k' = V_{k,Y}' + V_{k,T}' + V_{k,C}' \quad (2)$$

$V_{k,Y}'$ is the ordinary diffusion velocity given by the mixture-averaged formula [26]:

$$Y_k V_{k,Y}' = -D_{km}\frac{1}{\bar{M}}\frac{\partial(Y_k\bar{M})}{\partial r} \quad (3)$$

where Y_k is the mass fraction of species k; D_{km} is the mixture-averaged diffusion coefficient of species k; $\bar{M}$ is the mean molecular weight of the mixture; and r is the spherical coordinate. The coefficient D_{km} is explicitly determined from the binary diffusion coefficients D_{kj} [26]:

$$D_{km} = \frac{1-Y_k}{\sum_{j\neq k} X_j/D_{kj}} \quad (4)$$

where X_k is the molar fraction of species k. The binary diffusion coefficients D_{kj} are evaluated in CHEMKIN package based on classical kinetic theory [1].

$V_{k,T}'$ is the Soret/thermal diffusion velocity, which is proportional to the temperature gradient normalized by temperature itself:

$$Y_k V_{k,T}' = -D_{km}\Theta_k\frac{M_k}{\bar{M}T}\frac{\partial T}{\partial r} \quad (5)$$

where Θ_k and M_k are, respectively, the thermal diffusion ratio and molecular weight of species k. The correction velocity $V_{k,C}'$ is included to ensure the compatibility of species and mass conservation equations [26] and it is determined by the requirement of $\sum_{k=1}^{N}(Y_k V_k') = 0$ (where N is the total number of species). In the CHEMKIN package [26], the Wilke formula is used to determine the mixture viscosity and the mixture thermal conductivity is given in terms of the mass fractions and the thermal conductivity of each species. It is noted that the mixture-averaged model instead of the multi-component formulation is used here. Nevertheless, Bongers and De Goey [8] showed that for hydrogen/air and methane/air mixtures, there is negligible difference in the LFSs predicted by the mixture-averaged and multi-component models.

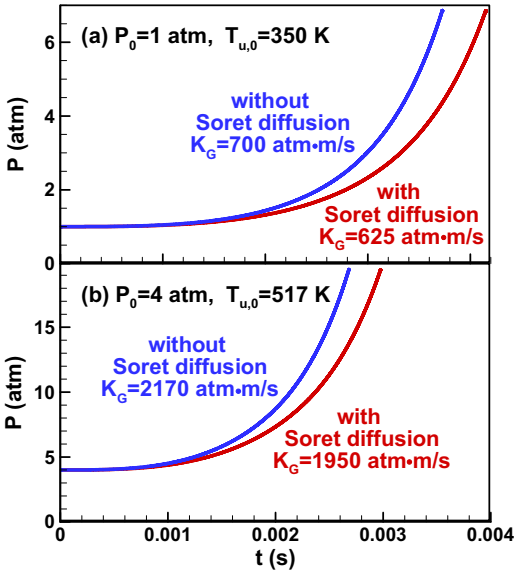

Fig. 1. Pressure rise history during spherical stoichiometric H_2/air flame propagating in a closed spherical vessel with $R_W = 5$ cm.

In simulation, the propagating spherical flame is initiated by a small hot pocket (around 1 mm in radius). The radius of the spherical vessel is $R_W = 5$ cm. Adaptive mesh refinement is used to accurately and efficiently resolve the propagating flame front. At high pressures, the smallest mesh size is 8 μm and grid convergence is achieved. The initial temperature of $T_0 = 350$ K, pressure of $P_0 = 1$ atm, and flow velocity of $u_0 = 0$ cm/s are uniformly distributed in the whole computational domain. To reach higher temperature and pressure in unburned gas during spherical flame propagation, the initial temperature and pressure are increased to the corresponding values after isentropic compression (e.g., 517 K and 4 atm for stoichiometric H_2/air as shown in Fig. 1b).

3. Results and discussion

We first consider spherical flame propagation in stoichiometric H_2/air mixture. Figure 1 shows the pressure rise history. The pressure rise becomes faster once Soret diffusion is neglected, indicating higher flame propagation speed for the case without Soret diffusion. Figure 1 also shows the values of the deflagration index, K_G, which is defined as maximum pressure rise rate multiplied by the cube root of volume, i.e., $K_G = (dP/dt)_{max}V^{1/3}$ [35,36]. The maximum pressure rise rate during gas explosions in enclosures, $(dP/dt)_{max}$, is an important parameter in explosion. However, $(dP/dt)_{max}$ depends not only on the mixture properties (such as mixture composition, initial temperature and initial pressure) but also on the volume of the vessel in which gas explosion takes place. Unlike $(dP/dt)_{max}$, the deflagration index K_G is an intrinsic property of the premixture and it is independent of the volume of the vessel used in experimental measurements. Therefore, it is popularly used to quantify the

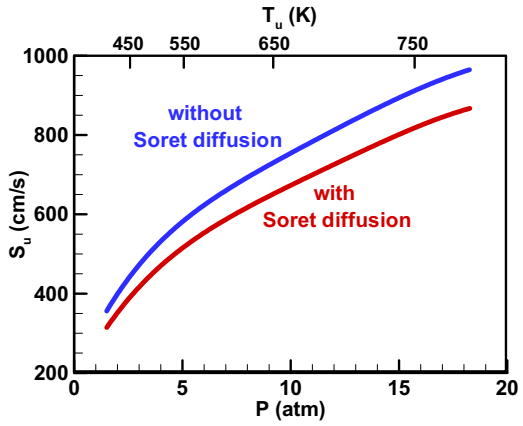

Fig. 2. Change of the laminar flame speed of stoichiometric H_2/air mixture with the pressure and temperature. The pressure and temperature satisfies the isentropic compression relationship with the initial values of $P = 1$ atm and $T_u = 350$ K.

potential severity of unwanted explosion [35,36]. The deflagration index is shown to be over-predicted by 11% when Soret diffusion is neglected. Therefore, Soret diffusion has strong impact on the pressure rise rate and deflagration index which are popularly used to quantify the potential severity of an explosion.

Figure 2 shows the LFS of stoichiometric H_2/air mixture with and without considering Soret diffusion. It is noted that during the isentropic compression, the temperature and pressure of unburned gas simultaneously increases and thereby both P and T_u are shown in Fig. 2. As expected, the inclusion of Soret diffusion always reduces the LFS. Such reduction in LFS monotonically increases with the initial pressure and temperature: it is 62 cm/s at $P = 4$ atm and $T_u = 517$ K, while it becomes 97 cm/s at $P = 18$ atm and $T_u = 781$ K. Simulations are also conducted for stoichiometric H_2/O_2 mixture. It is found that the impact of Soret diffusion on H_2/O_2 flames is also very important and that in terms of absolute reduction of LFS, the Soret effect on H_2/O_2 mixture is much larger than that for H_2/air mixture.

Usually the burning rate is quantified by the laminar burning flux (which is defined as $m = \rho_u S_u$, where ρ_u is the unburned gas density and S_u is the LFS) instead of LFS [1]. Since the unburned gas density significantly increases during the compression process, Soret diffusion has stronger influence on the laminar burning flux than on the LFS. This is demonstrated by Fig. 3 which shows the absolute and relative reduction in laminar burning flux due to Soret diffusion, δ_m and δ_m/m. The absolute reduction in laminar burning flux is defined as the difference of laminar burning flux with and without including Soret diffusion, i.e., $\delta_m = m_{\text{noSoretDiffusion}} - m_{\text{withSoretDiffusion}}$. It is observed that δ_m increases linearly with P (note that T_u also increases). We have $\delta_m = 0.12$ g/s/m^2 at $P = 4$ atm and $T_u = 517$ K. However, it is increased by around five times to $\delta_m = 0.57$ g/s/m^2 at $P = 18$ atm and $T_u = 781$ K. It also shows that the relative reduction, δ_m/m, slightly decreases as the pressure increases. Nevertheless, the relative reduction remains to be above 10%. Results for other equivalence ratios are also obtained, and similar trend is observed. Therefore, for H_2/air mixture, Soret diffusion has much stronger influence on burning rate at engine-relevant conditions than at normal temperature and pressure.

The change of Soret diffusion effects with the initial temperature and pressure was interpreted in [12] for syngas/air mixture. Similar interpretation can be conducted here for H_2/air mixture. The reduction of LFS was found to be induced mainly by the coupling between Soret diffusion of H radical and the chain branching reaction $H + O_2 = O + OH$ [9,12]. Such coupling is quantitatively

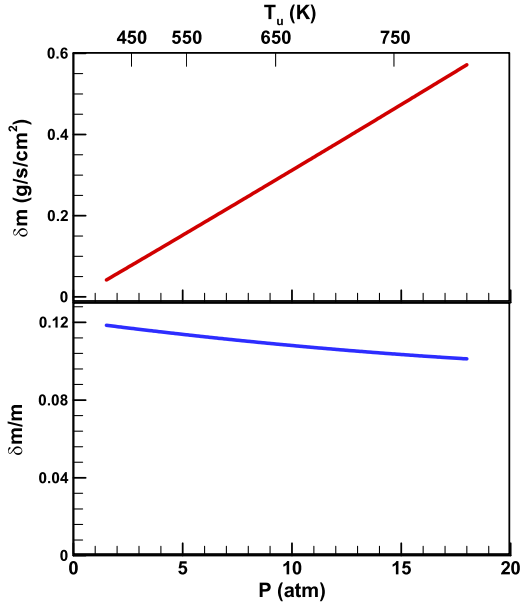

Fig. 3. The absolute and relative reduction in laminar burning flux due to Soret diffusion for stoichiometric H_2/air mixture.

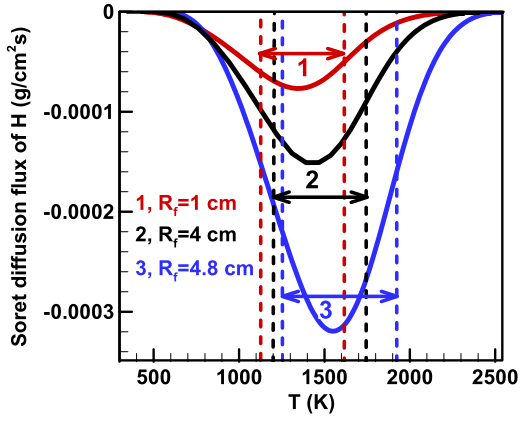

Fig. 4. Coupling between Soret diffusion of H radical and the chain branching reaction $H + O_2 = O + OH$ for spherical H_2/air flames at $R_f = 1$ cm ($T_u = 351$ K, $P = 1.01$ atm), 4 cm ($T_u = 430$ K, $P = 2.08$ atm), and 4.8 cm ($T_u = 543$ K, $P = 4.74$ atm). The solid lines represent Soret diffusion flux of H. At the temperature region denoted by the arrowed-lines between two vertical dashed lines, the reaction rate of $H + O_2 = O + OH$ is above 50% of its peak value.

demonstrated in Fig. 4. The Soret diffusion flux of H radical is defined as $\rho Y_H V'_{H,T}$, in which ρ is the density, Y_H is the mass fraction of H radical, and $V'_{H,T}$ is the Soret diffusion velocity given by Eq. (5). The main relevant reaction for H radical, $H + O_2 = O + OH$, is used to illustrate the major reaction zone. At the temperature region between two vertical lines shown in Fig. 4, the reaction rate of $H + O_2 = O + OH$ is above 50% of its peak value and thereby this region is referred to as the main reaction zone. Therefore, we need focus on the change of Soret diffusion of H radical only within the main reaction zone (i.e., between two vertical dashed lines). With the increase of initial temperature and pressure (from $T_u = 351$ K and $P = 1.01$ atm to $T_u = 430$ K and $P = 2.08$ atm, and to $T_u = 543$ K and $P = 4.74$ atm), Fig. 4 shows that Soret diffusion flux of H radical becomes larger. Meanwhile, the coupling between Soret diffusion of H radical and the chain branching reaction $H + O_2 = O + OH$ is shown to remain unchanged. Besides, Soret diffusion flux of H_2 is also found to increase with the initial temperature and pressure. Consequently, Fig. 4 helps to explain the observation that the

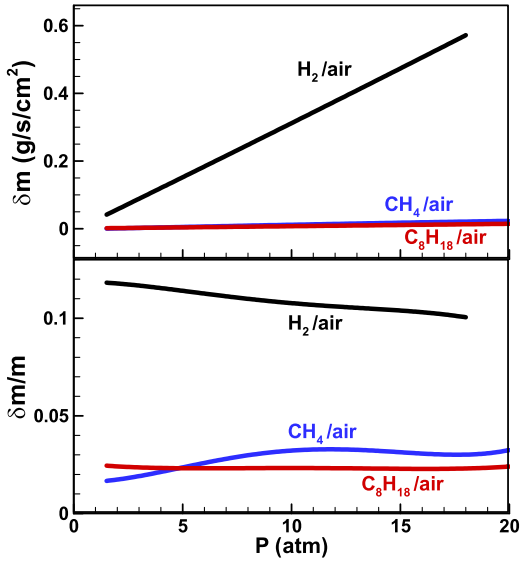

Fig. 5. The absolute and relative reduction in laminar burning flux due to Soret diffusion for stoichiometric H_2/air, CH_4/air and iC_8H_{18}/air flames. It is noted that the temperature increases with the pressure during the isentropic compression.

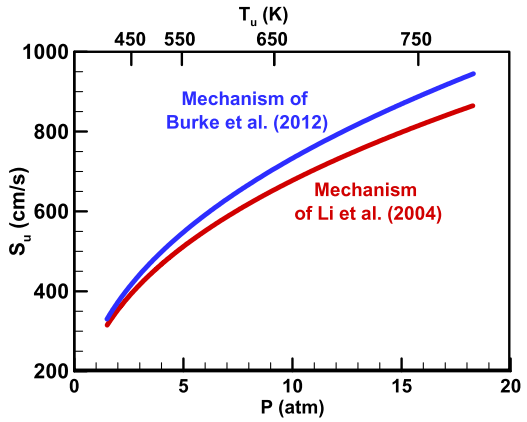

Fig. 6. Change of laminar flame speed of stoichiometric H_2/air mixture with the pressure and temperature. The pressure and temperature satisfies the isentropic compression relationship with the initial values of $P = 1$ atm and $T_u = 350$ K. The results are predicted by two hydrogen mechanisms by Li et al. [27] and Burke et al. [37].

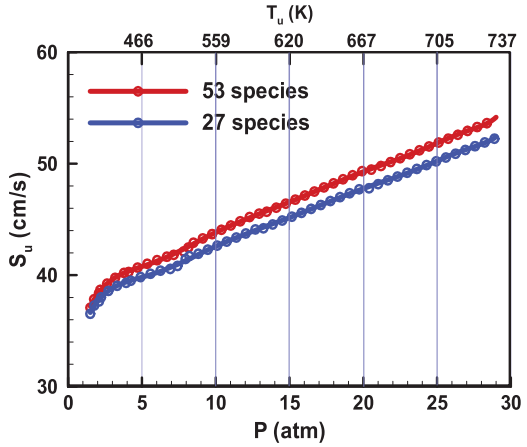

Fig. 7. Change of laminar flame speed of stoichiometric CH_4/air mixture with the pressure and temperature. The pressure and temperature satisfies the isentropic compression relationship with the initial values of $P = 1$ atm and $T_u = 300$ K. The results are predicted by original GRI Mech 3.0 with 53 species [28] and the reduced mechanism of 27 species [38].

higher initial temperature and pressure, the larger the reduction in LFS and laminar burning flux by Soret diffusion as shown in Figs. 2 and 3.

The influence of Soret diffusion on the LFS of stoichiometric CH_4/air and iC_8H_{18}/air at engine-relevant conditions is also examined. The results are shown in Fig. 5. Compared to H_2/air, the reduction in laminar burning flux of CH_4/air and iC_8H_{18}/air by Soret diffusion is shown to be negligible. In terms of relative reduction, it is below 3% for CH_4/air and iC_8H_{18}/air, which is much smaller than 10% for H_2/air. Therefore, similar to previous results at normal temperature and pressure [8,10,11], under engine-relevant conditions Soret diffusion effects on the burning rate of hydrocarbon fuels is still negligible. Besides, Fig. 5 shows that for H_2/air, the relative reduction in laminar burning flux by Soret diffusion slightly decreases but remains to be around 10% when the engine-relevant conditions are approached.

4. On calculating LFSs over a broad range of temperatures and pressures

Usually the CHEMKIN-PREMIX [22] is used to calculate the LFS. In each calculation, we can only obtain the LFS for one specific condition (i.e., at given initial temperature and pressure). Moreover, it is difficult to get converged solutions at high temperatures and pressures.

In the present work, the constant-volume propagating spherical flame in a closed vessel is simulated through A-SURF and then the LFSs over a broad range of temperatures and pressures can be obtained. In this method, LFS as a function of initial temperature (or pressure) can be obtained after running the code for one specific case (i.e., at given initial temperature and pressure). Therefore, this method is much more efficient than using CHEMKIN-PREMIX. Though the constant-volume propagating spherical flame method has been used by several groups in experiments measuring the LFS, it has not been used in simulations to calculate the LFS. This method has the advantage of obtaining LFSs at high temperatures and pressures close to engine-relevant conditions. Therefore, it is useful for comparing the performance of different mechanisms at elevated temperatures and pressures. Figure 6 compares the performance of two hydrogen mechanisms [27,37] in terms of predicting the LFSs of stoichiometric H_2/air over a broad range of temperatures and pressures. At low temperatures and pressures, there is little difference between the predictions by these two mechanisms. However, at elevated temperatures and pressures the difference becomes considerable.

Besides, this method can be used to assess the performance of reduced chemical mechanism over a broad range of temperatures and pressures. For example, Fig. 7 compares the performance of the reduced GRI mechanism with 27 species [38] with that of the original GRI mechanism [28] in terms of predicting the LFSs. It is observed that even at pressure close to 30 atm, the relative difference is still within 5%. Therefore, Fig. 7 indicates the reduced mechanism [38] yields good prediction for LFSs at high temperatures and pressures.

5. Conclusions

The effects of Soret diffusion on premixed flame propagation at engine-relevant temperatures and pressures are examined for different fuels. For H_2/air mixture, Soret diffusion reduces the pressure rise rate and LFS by around 10%. The reduction in laminar burning flux by Soret diffusion is shown to greatly increase with the initial temperature and pressure. This is mainly due to the fact that Soret diffusion flux of H and H_2 both increase with the

initial temperature and pressure. Therefore, Soret diffusion has much stronger influence on the burning rate at engine-relevant conditions than at normal temperature and pressure. However, for hydrocarbon fuels like methane and iso-octane, the effects of Soret diffusion on the burning rate is negligible even under engine-relevant conditions.

Acknowledgments

This work was supported by National Natural Science Foundation of China (Nos. 91541204 and 91741126) and National Program for Support of Top-notch Young Professionals. We thank Mr. Yiqing Wang at Peking University for providing Fig. 7.

Supplementary materials

Supplementary material associated with this article can be found, in the online version, at doi:10.1016/j.combustflame.2018.04.031.

References

[1] C.K. Law, Combustion physics, Cambridge University Press, New York, USA, 2006.
[2] J. Hirschfelder, R.B. Bird, C.F. Curtiss, Molecular theory of gases and liquids, John Wiley, 1954.
[3] A.L. Sánchez, F.A. Williams, Recent advances in understanding of flammability characteristics of hydrogen, Prog. Energy Combust. Sci. 41 (2014) 1–55.
[4] V. Giovangigli, Multicomponent transport in laminar flames, Proc. Combust. Inst. 35 (2015) 625–637.
[5] W. Han, Z. Chen, Effects of Soret diffusion on laminar flames (in Chinese), Sci. Sin. Tech. 45 (2015) 1117–1129.
[6] A. Ern, V. Giovangigli, Thermal diffusion effects in hydrogen-air and methane-air flames, Combust. Theor. Model. 2 (1998) 349–372.
[7] A. Ern, V. Giovangigli, Impact of detailed multicomponent transport on planar and counterflow hydrogen/air and methane/air flames, Combust. Sci. Technol. 149 (1999) 157–181.
[8] H. Bongers, L.P.H. De Goey, The effect of simplified transport modeling on the burning velocity of laminar premixed flames, Combust. Sci. Technol. 175 (2003) 1915–1928.
[9] F. Yang, C.K. Law, C.J. Sung, H.Q. Zhang, A mechanistic study of Soret diffusion in hydrogen–air flames, Combust. Flame 157 (2010) 192–200.
[10] F. Yang, H.Q. Zhang, X.L. Wang, Effects of soret diffusion on the laminar flame speed of n-butane-air mixtures, Proc. Combust. Inst. 33 (2011) 947–953.
[11] Y. Xin, C.-J. Sung, C.K. Law, A mechanistic evaluation of Soret diffusion in heptane/air flames, Combust. Flame 159 (2012) 2345–2351.
[12] W. Liang, Z. Chen, F. Yang, H. Zhang, Effects of Soret diffusion on the laminar flame speed and Markstein length of syngas/air mixtures, Proc. Combust. Inst. 34 (2013) 695–702.
[13] P. GarcÍA-Ybarra, C. Nicoli, P. Clavin, Soret and dilution effects on premixed flames, Combust. Sci. Technol. 42 (1984) 87–109.
[14] W. Han, Z. Chen, Effects of Soret diffusion on premixed counterflow flames, Combust. Sci. Technol. 187 (2015) 1195–1207.
[15] W. Han, Z. Chen, Effects of Soret diffusion on spherical flame initiation and propagation, Int. J. Heat Mass Transf. 82 (2015) 309–315.
[16] Z. Zhou, F.E. Hernández-Pérez, Y. Shoshin, J.A. van Oijen, L.P.H. de Goey, Effect of Soret diffusion on lean hydrogen/air flames at normal and elevated pressure and temperature, Combust. Theor. Model. 21 (2017) 879–896.
[17] M. Faghih, Z. Chen, The constant-volume propagating spherical flame method for laminar flame speed measurement, Sci. Bull. 61 (2016) 1296–1310.
[18] C. Xiouris, T. Ye, J. Jayachandran, F.N. Egolfopoulos, Laminar flame speeds under engine-relevant conditions: Uncertainty quantification and minimization in spherically expanding flame experiments, Combust. Flame 163 (2016) 270–283.
[19] S.P. Marshall, S. Taylor, C.R. Stone, T.J. Davies, R.F. Cracknell, Laminar burning velocity measurements of liquid fuels at elevated pressures and temperatures with combustion residuals, Combust. Flame 158 (2011) 1920–1932.
[20] O. Askari, A. Moghaddas, A. Alholm, K. Vien, B. Alhazmi, H. Metghalchi, Laminar burning speed measurement and flame instability study of H_2/CO/air mixtures at high temperatures and pressures using a novel multi-shell model, Combust. Flame 168 (2016) 20–31.
[21] Z. Chen, On the accuracy of laminar flame speeds measured from outwardly propagating spherical flames: methane/air at normal temperature and pressure, Combust. Flame 162 (2015) 2442–2453.
[22] R.J. Kee, J. Grcar, M. Smooke, J. Miller, PREMIX: a FORTRAN program for modeling steady laminar one-dimensional premixed flames, 1985 Sandia National Laboratories Report. SAND85-8240.
[23] Z. Chen, M.P. Burke, Y.G. Ju, Effects of Lewis number and ignition energy on the determination of laminar flame speed using propagating spherical flames, Proc. Combust. Inst. 32 (2009) 1253–1260.
[24] Z. Chen, Effects of radiation and compression on propagating spherical flames of methane/air mixtures near the lean flammability limit, Combust. Flame 157 (2010) 2267–2276.
[25] P. Dai, Z. Chen, Supersonic reaction front propagation initiated by a hot spot in n-heptane/air mixture with multistage ignition, Combust. Flame 162 (2015) 4183–4193.
[26] R.J. Kee, F. Rupley, J. Miller, CHEMKIN-II: a FORTRAN chemical kinetics package for the analysis of gas-phase chemical kinetics, 1993 Sandia National Laboratories Report. SAND89-8009B.
[27] J. Li, Z. Zhao, A. Kazakov, F.L. Dryer, An updated comprehensive kinetic model of hydrogen combustion, Int. J. Chem. Kinet. 36 (2004) 566–575.
[28] G. Smith, D. Golden, M. Frenklach et al., The GRI-Mech 3.0 chemical kinetic mechanism. http://combustion.berkeley.edu/gri-mech/.
[29] M. Chaos, A. Kazakov, Z. Zhao, F.L. Dryer, A high-temperature chemical kinetic model for primary reference fuels, Int. J. Chem. Kinet. 39 (2007) 399–414.
[30] H. Yu, Z. Chen, End-gas autoignition and detonation development in a closed chamber, Combust. Flame 162 (2015) 4102–4111.
[31] P. Dai, Z. Chen, S. Chen, Y. Ju, Numerical experiments on reaction front propagation in n-heptane/air mixture with temperature gradient, Proc. Combust. Inst. 35 (2015) 3045–3052.
[32] Z. Chen, Effects of radiation absorption on spherical flame propagation and radiation-induced uncertainty in laminar flame speed measurement, Proc. Combust. Inst. 36 (2017) 1129–1136.
[33] H. Yu, C. Qi, Z. Chen, Effects of flame propagation speed and chamber size on end-gas autoignition, Proc. Combust. Inst. 36 (2017) 3533–3541.
[34] M. Faghih, Z. Chen, Two-stage heat release in nitromethane/air flame and its impact on laminar flame speed measurement, Combust. Flame 183 (2017) 157–165.
[35] D.A. Crowl, Understanding explosions, John Wiley & Sons, 2010.
[36] M. Faghih, X. Gou, Z. Chen, The explosion characteristics of methane, hydrogen and their mixtures: a computational study, J. Loss Prev. Process Ind 40 (2016) 131–138.
[37] M.P. Burke, M. Chaos, Y. Ju, F.L. Dryer, S.J. Klippenstein, Comprehensive H_2/O_2 kinetic model for high-pressure combustion, Int. J. Chem. Kinet. 44 (2012) 444–474.
[38] Y. Chen, J.-Y. Chen, Towards improved automatic chemical kinetic model reduction regarding ignition delays and flame speeds, Combust. Flame 190 (2018) 293–301.